

RSC Advances



This is an *Accepted Manuscript*, which has been through the Royal Society of Chemistry peer review process and has been accepted for publication.

Accepted Manuscripts are published online shortly after acceptance, before technical editing, formatting and proof reading. Using this free service, authors can make their results available to the community, in citable form, before we publish the edited article. This *Accepted Manuscript* will be replaced by the edited, formatted and paginated article as soon as this is available.

You can find more information about *Accepted Manuscripts* in the [Information for Authors](#).

Please note that technical editing may introduce minor changes to the text and/or graphics, which may alter content. The journal's standard [Terms & Conditions](#) and the [Ethical guidelines](#) still apply. In no event shall the Royal Society of Chemistry be held responsible for any errors or omissions in this *Accepted Manuscript* or any consequences arising from the use of any information it contains.

Strain-Mediated Multilevel Ferroelectric Random Access Memory Operating through a Magnetic Field

Jie Wang^{a,b,*}, Koyo Nagano^b, Takahiro Shimada^{b,#}, and Takayuki Kitamura^b

^a*Department of Engineering Mechanics, School of Aeronautics and Astronautics,
Zhejiang University, Hangzhou 310027, China*

^b*Department of Mechanical Engineering and Science, Kyoto University,
Nishikyo-ku, Kyoto 615-8540, Japan*

Abstract

Ferroelectric random access memory (FeRAM) is based on the physical movement of atoms in response to external fields, which has lower power consumption and faster writing performance than conventional flash memory. However, the wide application of current FeRAM is limited by its low storage density. Here we demonstrate, using phase field simulations, a new pathway towards high-density multilevel FeRAM that exhibits significant improvement over the one level FeRAM technologies. The proposed multilevel FeRAM devices employ the strain-mediated multiple vortex states of polarization to store more information, which is based on the novel switching behavior between the single and triple vortex states under a time-dependent magnetic field. The FeRAM can store two bits per cell via four stable vortex states of polarization. As a consequence, the areal bit densities of the polarization vortex states of the FeRAM can be two times higher than those of the one level FeRAM employing single vortex state of polarization.

* E-mail: jw@zju.edu.cn

#E-mail: shimada@me.kyoto-u.ac.jp

Introduction

Ferroelectric random access memory (FeRAM) uses two opposite states of polarization to store information. An external electric field can switch the polarization between the “up” and “down” states¹, representing “0” and “1”. Because of its low power consumption², fast write performance³, and a great maximum number of write-erase cycles⁴, FeRAM becomes a promising candidate as a solid state universal memory⁵. However, the ferroelectrics tend to stop being in the ferroelectric or rectilinear state when they are too small⁶, and it is difficult to reduce the feature cell size of the ferroelectric memory compared to other universal memory candidates⁷⁻¹¹. As a result, despite its great promise, the widely commercial application of FeRAM is limited by its low storage density¹². A breakthrough for addressing this critical issue of low density in FeRAM may be possible through a multilevel operation¹³⁻¹⁵ and using a new order parameter to store information^{16,17}.

Due to the depolarization effect, ferroelectrics at the nanometer scale, including ferroelectric nanodisks¹⁷, nanodots^{18,19}, and nanotubes^{20,21}, exhibit a novel toroidal order of polarization, in which polarization vectors form a vortex structure with the head-to-tail polarization arrangement and a zero total net polarization. The polarization vortex is defined as a new order parameter by the toroidal moment of polarization of $\mathbf{G} = \frac{1}{V} \int_V \mathbf{r} \times \mathbf{P} dV$, where \mathbf{P} and \mathbf{r} are the polarization and position vectors, respectively¹⁷. The polarization vortex has two stable states (clockwise and counterclockwise circulations), which can be switched from one state to the other by a time-dependent magnetic field. The bistable property of the toroidal moment of polarization can potentially be applied to store information. The advantage of using the toroidal moment of polarization as a data bit over the rectilinear state of polarization is that the former can be stable in a much smaller size than the latter, resulting in a higher storage density of the FeRAM¹⁷.

On the other hand, phase field simulations show that a transformation from the single-vortex state to a multivortex state in the ferroelectric nanostructures subjected to a mechanical load exists²². Controllable transformation between the multi- and single-vortex states can provide reliable multilevel toroidal moments, offering a unique opportunity for multilevel memory. Unlike a single-level memory cell, which can only store 1 bit per cell and is always in one of two states, programmed (0) or erased (1), a multilevel memory cell has more than two states, because each bit in the cell is either programmed or erased. The double-level cell, for example, has four states (00, 01, 10, and 11), which can store 2 bits per cell. The combination of the multilevel operation and toroidal order of polarization in FeRAM holds the promise to double the storage density of the one level FeRAM that employs the single vortex state of polarization.¹⁷

In this study, we introduce a simple and new approach towards high-density multilevel FeRAM that employs the multiply stable vortex states of polarization to store information operated by a time-dependent magnetic field. Due to the presence of the compressive strain, the switching between the single and triple vortex states takes place under a curled electric field. Switching among the four stable vortex states of polarization suggests that each cell can store two bits. Therefore, the density of the proposed multilevel FeRAM is two times higher than that of one level FeRAM based on the single polarization vortex.

Results and discussion

Fig. 1a shows a three-dimensional schematic diagram of a multilevel memory cell array based on the polarization vortex. The ferroelectric memory cells are built on a dielectric substrate and separated by dielectric blocks. A uniaxial compressive strain in the ferroelectric memory cells is generated and maintained

through the lattice mismatch²³ between the ferroelectric memory cells and the underlying dielectric substrate. The permittivity of dielectric substrate is assumed much smaller than that of the ferroelectric memory cells, and thus the interface between the cells and substrate can be regarded as open-circuited. Due to the open-circuited boundary condition on the surfaces and interfaces, polarization vectors will form a vortex structure in the ferroelectric memory cells. In particular, multivortex states could appear when the memory cells are subjected to a compressive strain. Four stable vortex states, including two single-vortex states and two multivortex states (see the arc arrows in Fig. 1a) are possible in the ferroelectric memory cells under the compressive strain. Furthermore, these stable vortex states can be switched from one to the other by applying an appropriate time-dependent magnetic field, which offers a unique opportunity for developing multilevel memory.

The switching between different states of a polarization vortex is the basis of the application of a vortex state in nonvolatile random access memories. Studies based on the atomistic first-principles derived effective Hamilton method²⁴ and continuum phase field model^{19,21} show that the switching of the polarization vortex is completely different from the polarization switching under a uniform electric field in traditional capacitor-type ferroelectrics. The switching process of a polarization vortex can be completed by a curled electric field²¹, which is generated by a time-dependent magnetic field through the Maxwell equations, as shown in Fig. 1b. Compared with the one level FeRAM based on single polarization vortex, the present multilevel FeRAM has four stable polarization vortex states in the absence of external electric field, which can be used to store two data bits per cell. As a result, the storage density of the proposed multilevel FeRAM is two times higher than that of one level FeRAM based on the single polarization vortex. Furthermore, the time dependent magnetic field is perpendicular to the surface of the bit cell, which is similar to current perpendicular magnetic storage technology²⁵. Therefore, the writing and reading system of the FeRAM of polarization vortex is compatible with current perpendicular magnetic memory, which makes the proposed

FeRAM applicable to practical uses and reduces the design cost.

When a time-dependent magnetic field is applied perpendicularly to the polarization vortex, a curled electric field is generated according to the Maxwell equation, $\nabla \times \mathbf{E}^{Cur} = -\frac{\partial \mathbf{B}(t)}{\partial t}$, where \mathbf{E}^{Cur} and $\mathbf{B}(t)$ are the curled electric field and time-dependent magnetic field, respectively. The polarization vortex could be switched if the curled electric field is antiparallel to the polarizations and exceeds a critical value. Correspondingly, the toroidal moment of polarization, \mathbf{G} , is switched by the time-dependent magnetic field. The change rate of the magnetic field with time is associated with the vorticity of the curled electric field as $\mathbf{S} = -\frac{\partial \mathbf{B}(t)}{\partial t}$, which is a thermodynamically conjugated field to the toroidal moment of polarization. Analogous to the common P-E hysteresis loop of ferroelectrics, Fig. 2 shows the response of the toroidal moment \mathbf{G} to a cycling vorticity \mathbf{S} in the x_3 direction at room temperature in the ferroelectric memory cell subjected to different compressive strains. When the compressive strain is small, the G-S hysteresis loop has a good rectangular shape, as shown in Fig. 2a for the compressive strain of $\varepsilon_{11} = -0.005$, which is desirable for memory applications. The polarizations form a single vortex, which is similar to that in nanodots without a mechanical load¹⁸, indicating that the present simulation is reliable. In the absence of a curled electric field, the single vortex can be clockwise or counterclockwise, which generates a positive or negative toroidal moment at $S=0$ in the curve of hysteresis loop, respectively. When the compressive strain increases to -0.01, the critical vorticity that switches the vortex becomes smaller due to the formation of an intermediate triple-vortex state at point C, as shown by the curve in Fig. 2b. The appearance of an intermediate triple-vortex state at a smaller vorticity indicates the influence of elastic energy. When the compressive strain further increases, the single-vortex state becomes unstable, while the multivortex states are more energetically favorable. Thus, a very small curled field can induce a transformation from the single-vortex state to the triple-vortex state, as shown by

the sudden drop of toroidal moment in Fig. 2c for the strain of -0.012. The multivortex state often results in a smaller toroidal moment for a cell with the same size due to the cancelation of toroidal moments between different vortices. Furthermore, the single vortex does not appear in a wide range of vorticity under a large strain, which is shown by the small toroidal moment between -0.1 and 0.1 in Fig. 2d for the strain of -0.025. The strain dependence of the G-S hysteresis loop indicates that a small compressive strain prefers a single-vortex state, while a large one induces a multivortex state, which is consistent with a previous study²⁶. It should be noted that both the single- and triple-vortex states can exist under a moderate strain in the present study. In addition, the transformation between the single- and triple-vortex states can be induced by a curled electric field, implying that the multilevel toroidal moments can be controlled by a time-dependent magnetic field.

To realize the control of multilevel toroidal moments by using a time-dependent magnetic field, the ferroelectric memory cell with a moderate strain of -0.01 was investigated by applying different vorticities. When the vorticity is cycled between points E and K, a large hysteresis loop between the toroidal moment G and vorticity S is obtained, as shown by the curve of B-C-D-E-H-I-J-K in Fig. 3a, which is the enlarged curve of Fig. 2b. In the hysteresis loop, the single vortex formed at two stable states of points A and G with $S=0$, which are shown by Fig. 3b. The counterclockwise single-vortex state at point A can be switched to the clockwise single-vortex state at point E along the path A-B-C-D-E when the negative vorticity increases. During the switching process, there are two intermediate triple-vortex states at points C and D. The switching from the single vortex at point B to the triple vortex at point C is initiated by the disappearance of polarizations at the mid-sections of the upper and lower surfaces under the external strain, as shown in Fig. 4. Interestingly, the intermediate triple state at point C in Fig. 3a does not return to the initial single-vortex state when the

negative vorticity decreases from point C to zero. Correspondingly, the toroidal moment does not decrease along the original path C-B-A, but along a new path C-M as shown in Fig. 3a. When the vorticity decreases to zero, the toroidal moment becomes $0.2 \text{ e}/\text{\AA}$ at point M, which is much smaller than $0.9 \text{ e}/\text{\AA}$ at point A. The smaller toroidal moment is attributed to the fact that the triple-vortex structure is retained along the path C-M, as shown in Fig. 5. The toroidal moment increases when the vorticity increases from points M to P. The polarizations still form a triple-vortex structure although the middle vortex is smaller than the other two vortices. If the vorticity further increases to point L, the triple-vortex state will become a counterclockwise single-vortex state, which has a similar polarization distribution as point A. However, the triple vortex will remain and return back to point M when the vorticity decreases from point P to zero. The transition between different vortex states is highly dependent on the loading path. The triple-vortex state will transfer into a clockwise single-vortex state at point E when the negative vorticity increases along the path of M-C-D-E. When the vorticity cycles are between points F and I, the toroidal moment will change along the path of F-E-G-H-I and then come back along the path of I-N-O-F. As a result, a small hysteresis loop between the toroidal moment and vorticity is obtained below the line of $G=0$. Similarly, a small hysteresis loop exists between points L and C above the line of $G=0$. In the small hysteresis loops, two stable triple-vortex states are obtained separately at points M and N, which are significantly different from the two single-vortex states at points A and G, as shown in Figs. 3b. Based on the hysteresis loops, four stable vortex states can be switched from one to the other by changing the vorticity (or the rate of the magnetic field) along different loading paths, as indicated by the arrows in Fig. 3, and thus the reading and writing of four vortex states of polarization can be achieved for two data bits in a single memory cell. At a constant vorticity, the writing speed of the FeRAM is dependent on the relaxation time of ferroelectric polarization. For a larger vorticity, the relaxation will be faster. Therefore, the higher the rate of magnetic field, the faster the writing speed of

the FeRAM.

For nonvolatile memory applications, the stability of the polarization vortex is important when the external field is absent. The formation of the vortex states of polarization involves intriguing competition between the elastic, depolarization, and gradient energies. The vortex state of polarization has low depolarization energy, but the elastic and gradient energies are high due to the inhomogeneous spontaneous polarization and lattice distortion. Although the appearance of different vortex states in the cell is dependent on the initial configuration or loading path, the minimization of total energy of the ferroelectric memory cell determines the final stable state of the polarization vortex. Fig. 6 provides the total energies of the different vortex states that can exist in a ferroelectric memory cell with different compressive strains in the absence of vorticity. Compared to the triple-vortex state, the single-vortex state has a lower energy when the strain is small. However, the energy of the single vortex increases quickly when the mechanical compressive strain increases. At the compressive strain of -0.013, it approaches the total energy of triple vortices. Correspondingly, the single vortex becomes unstable and vanishes when the compressive strain further increases. For the single-vortex state, 90° domain walls appear in the closure domain structure to reduce the elastic energy and depolarization energy, as shown in Fig. 3a. Most polarizations are parallel to the direction of the applied uniaxial strain. When the compressive strain increases, more polarizations become perpendicular to the direction of the applied uniaxial strain to further release the elastic energy. As a result, a triple-vortex state is formed under large compressive strains, although the gradient energy simultaneously increases. Despite the energy of a single vortex being lower than that of triple vortices, Fig. 6 confirms that both the single vortex and multivortex can exist in the ferroelectric memory cell when the compressive strain is in a range between 0 and -0.013. It is the coexistence of single- and multivortex states in a range of strain that provides the

opportunity for the transformation between the different vortex states under the external field.

Conclusion

We demonstrate here a simple and novel approach to create a nonvolatile high-density multilevel FeRAM technology that uses the strain-mediated multiple polarization vortices in ferroelectrics. It should be noted that the results reported here are obtained by using typical PbTiO_3 ferroelectric material and a specific cell size as proof of a practical concept. Further optimization on the applied strain and selection of cell materials could further reduce the cell size and increases the number of vortex states for a higher storage density. Compared with the one level FeRAM based on the single polarization vortex, the multilevel polarization vortex FeRAM reported here has a much higher density. Furthermore, it is operated through a time-dependent magnetic field, which is compatible with the currently used perpendicular magnetic memory, making the FeRAM applicable to practical uses and reduces the design cost. Therefore, it is expected that our results will stimulate further experimental and engineering efforts on developing multilevel high-density FeRAM devices.

Methods

Phase field method for ferroelectrics. In the phase field model, the electrical enthalpy density is described in terms of a set of spatially continuous but inhomogeneous polarization \mathbf{P} , strain $\boldsymbol{\varepsilon}$, polarization gradient $\nabla \cdot \mathbf{P}$, and electric field \mathbf{E} , which can be expressed as

$$h = f_{Lan}(\mathbf{P}) + f_{Ela}(\mathbf{P}, \boldsymbol{\varepsilon}) + f_{Gra}(\nabla \cdot \mathbf{P}) + f_{Ele}(\mathbf{E}, \mathbf{P}) \quad (1)$$

The first term on the right-hand side of Eq. (1) represents the Landau-Devonshire free-energy density. The second term is the energy related to strain, including the pure elastic energy density and the coupling energy density between the strain and polarization. The third term is the gradient energy, which gives the energy

penalty due to the spatially inhomogeneous polarization. The last term is the electric energy density in the presence of the electric field. The detailed expressions of these energy terms are the same as those given in Ref. [27]. The temporal evolution of the spatially inhomogeneous polarization is obtained by solving the time-dependent Ginzburg-Landau TDGL equation²⁸:

$$\frac{\partial P_i(\mathbf{r},t)}{\partial t} = -L \frac{\delta F}{\delta P_i(\mathbf{r},t)} \quad (i=1, 2, 3), \quad (2)$$

where L is the kinetic coefficient and $F = \int_V \Psi dv$ is the total free energy of the simulated system. The free-energy density Ψ is related to the electrical (Gibbs) enthalpy density h by the Legendre transformation $h = \Psi - D_i E_i$, where D_i and E_i are the electric displacement and electric field components, respectively. $\delta F / \delta P_i(\mathbf{r},t)$ represents the thermodynamic driving force for the spatial and temporal evolution of the polarizations, \mathbf{r} denotes the spatial vector, $\mathbf{r} = (x_1, x_2, x_3)$, and t is time. In addition to Eq. (2), the mechanical equilibrium equation $\sigma_{ij,j} = 0$ and the Gauss law $D_{i,i} = 0$ must be simultaneously satisfied, since the ferroelectric memory cell is charge-free and body-force-free. The stress and electric displacement are derived from $\sigma_{ij} = \partial h / \partial \varepsilon_{ij}$ and $D_i = -\partial h / \partial E_i$, respectively.

Magnetic field induced polarization switching. In the simulations, all surfaces and interfaces of the ferroelectric memory cell were assumed to be open-circuited, which is a necessary electrical boundary condition for the formation of a polarization vortex. The strain is applied by deforming the ferroelectric cell under an equivalent stress in the x_1 direction. The time-dependent Ginzburg-Landau TDGL equation, mechanical equilibrium equation, and Gauss' equation are solved by a nonlinear finite element method²⁹. We employed 2048 discrete brick elements to model the ferroelectric memory cell with 32, 16, and 4 elements in the x_1 , x_2 , and x_3 directions, respectively. The height of the simulated memory cell is 3 nm

and the in-plane sizes are 26×13 nm. All the material constants used in the simulation are the same as those of Ref. [19]. To avoid the numerical divergence, all the materials parameters are normalized as in Ref. [29] and the normalized equations are solved in the simulation. The electric field \mathbf{E} in Eq. (1) includes a common depolarization field \mathbf{E}^{Unc} (uncurled field) and an applied curled electric field \mathbf{E}^{Cur} , i.e., $\mathbf{E} = \mathbf{E}^{Unc} + \mathbf{E}^{Cur}$. The curled electric field is applied to the ferroelectric memory cell as $\nabla \times \mathbf{E}^{Cur} = -\frac{\partial \mathbf{B}(t)}{\partial t} = \mathbf{S}$, where \mathbf{S} is the vorticity vector. When a time-dependent magnetic field is applied perpendicular to the polarization vortex, the toroidal moment G changes correspondingly, resulting in a hysteresis loop of G and S in the x_3 direction.

Acknowledgements

The work was financially supported by Grants-in-Aid for Scientific Research(s) (Nos. 21226005 and 25000012) and a Research Fellowship (No. P12058) from the Japan Society of the Promotion of Science, and by the National Natural Science Foundation of China (Nos. 11090333, 11472242 and 11321202).

Notes and References

1. Lines, M. E. & Glass, A. M. *Principles and applications of ferroelectrics and related materials*. Clarendon: Oxford University Press (1977).
2. Scott, J. Applications of modern ferroelectrics. *Science* **315**, 954-959 (2007).
3. Rana, D. S. *et al.* Understanding the nature of ultrafast polarization dynamics of ferroelectric memory in the multiferroic BiFeO₃. *Adv. Mater.* **21**, 2881-2885 (2009).
4. Park, B. *et al.* Lanthanum-substituted bismuth titanate for use in non-volatile memories. *Nature* **401**, 682-684 (1999).
5. Scott, J. F. & De Araujo, C. A. P. Ferroelectric memories. *Science* **246**, 1400-1405 (1989).
6. Ahn, C., Rabe, K. & Triscone, J. M. Ferroelectricity at the nanoscale: local polarization in oxide thin films and heterostructures. *Science* **303**, 488-491 (2004).

7. Wuttig, M. & Yamada, N. Phase-change materials for rewriteable data storage. *Nat. Mater.* **6**, 824-832 (2007).
8. Chappert, C., Fert, A. & Van Dau, F. N. The emergence of spin electronics in data storage. *Nat. Mater.* **6**, 813-823 (2007).
9. Hu, J. M., Li, Z., Chen, L. Q. & Nan, C.W. High-density magnetoresistive random access memory operating at ultralow voltage at room temperature. *Nat. Commun.* **2**, 553 (2011).
10. Åkerman, J. Toward a universal memory. *Science* **308**, 508-510 (2005).
11. Miao, H.C et al, Magnetic-field-induced ferroelectric polarization reversal in magnetoelectric composites revealed by piezoresponse force microscopy. *Nanoscale*, **6**, 8515-8520 (2014).
12. Meijer, G. I. Who wins the nonvolatile memory race? *Science* **319**, 1625-1626(2008).
13. Lee, D. Multilevel data storage memory using deterministic polarization control. *Adv. Mater.* **24**, 402-406 (2012).
14. Lee, J. S. *et al.* Multilevel data storage memory devices based on the controlled capacitive coupling of trapped electrons. *Adv. Mater.* **23**, 2064-2068 (2011).
15. Zhou, Y., Han, S. T., Sonar, P. & Roy, V. Nonvolatile multilevel data storage memory device from controlled ambipolar charge trapping mechanism. *Scientific Report* **3**, 2319(2013).
16. Guo, R. *et al.* Non-volatile memory based on the ferroelectric photovoltaic effect. *Nat. Commun.* **4** (2013).
17. Naumov, I. I., Bellaiche, L. & Fu, H. Unusual phase transitions in ferroelectric nanodisks and nanorods. *Nature* **432**, 737-740 (2004).
18. Rodriguez, B. *et al.* Vortex polarization states in nanoscale ferroelectric arrays. *Nano lett.* **9**, 1127-1131 (2009).
19. Wang, J. Switching mechanism of polarization vortex in single-crystal ferroelectric nanodots. *Appl. Phys. Lett.* **97**, 192901 (2010).
20. Shimada, T., Wang, X., Kondo, Y. & Kitamura, T. Absence of Ferroelectric Critical Size in Ultrathin PbTiO₃ Nanotubes: A Density-Functional Theory Study. *Phys. Rev. Lett.* **108**, 067601 (2012).
21. Wang, J. & Kamlah, M. Intrinsic switching of polarization vortex in ferroelectric nanotubes. *Phys. Rev. B* **80**, 012101 (2009).
22. Chen, W., Zheng, Y. & Wang, B. Phase field simulations of stress controlling the vortex domain structures in ferroelectric nanosheets. *Appl. Phys. Lett.* **100**, 062901 (2012).
23. Schlom, D.G. Strain Tuning of Ferroelectric Thin Films. *Annu. Rev. Mater. Res.* **37**,589–626 (2007).
24. Naumov, I. I. & Fu, H. Cooperative response of Pb (ZrTi) O₃ nanoparticles to curled electric fields. *Phys. Rev. Lett.* **101**, 197601 (2008).
25. Litvinov, D. & Khizroev, S. Perpendicular magnetic recording: playback. *J. Appl. Phys.* **97**, 071101 (2005).

26. Chen, W., Zheng, Y. & Wang, B. Vortex domain structure in ferroelectric nanoplatelets and control of its transformation by mechanical load. *Scientific Report* **2**, 796 (2012).
27. Wang, J. & Kamlah, M. Domain structures of ferroelectric nanotubes controlled by surface charge compensation. *Appl. Phys. Lett.* **93**, 042906 (2008).
28. Chen, L. Q. Phase - Field Method of Phase Transitions/Domain Structures in Ferroelectric Thin Films: A Review. *J. Am. Ceram. Soc.* **91**, 1835-1844 (2008).
29. Wang, J. & Kamlah, M. Three-dimensional finite element modeling of polarization switching in a ferroelectric single domain with an impermeable notch. *Smart Mater. Struct.* **18**, 104008 (2009).

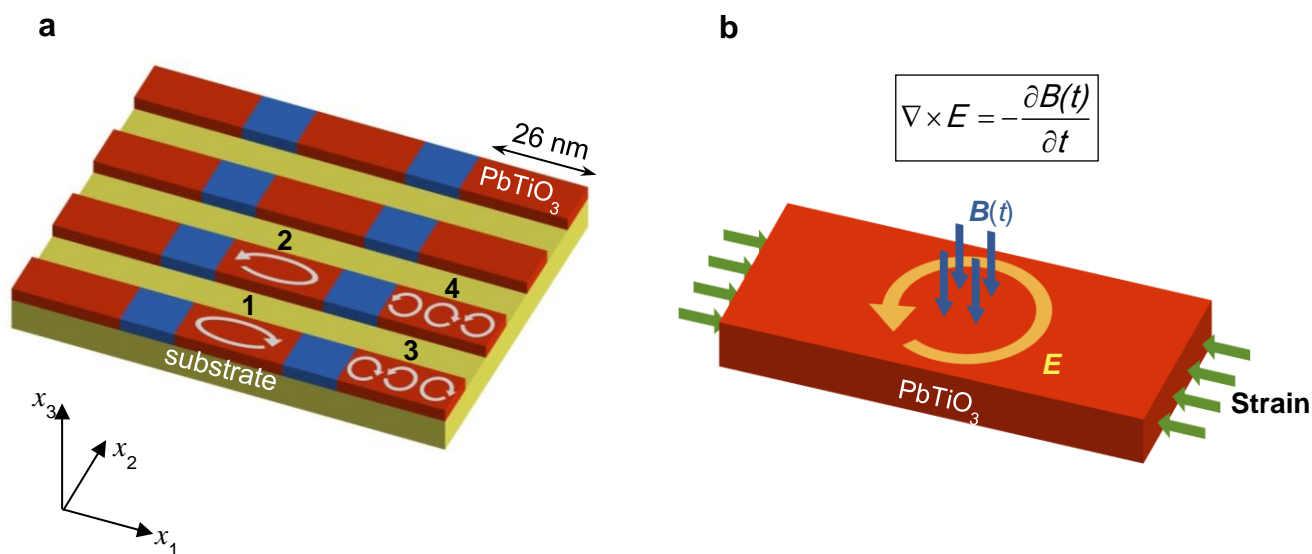


Figure 1 | **a** Three-dimensional schematic diagram of a multilevel memory cell array based on the polarization vortex. The ferroelectric PbTiO_3 memory cells are built on a dielectric substrate and separated by dielectric blocks. The dielectric blocks provide a uniaxial compressive strain on the ferroelectric memory cells via the misfit of thermal expansion between the ferroelectric and dielectric materials. **b** A perpendicular time-dependent magnetic field generates a curled electric field to switch the polarization vortex.

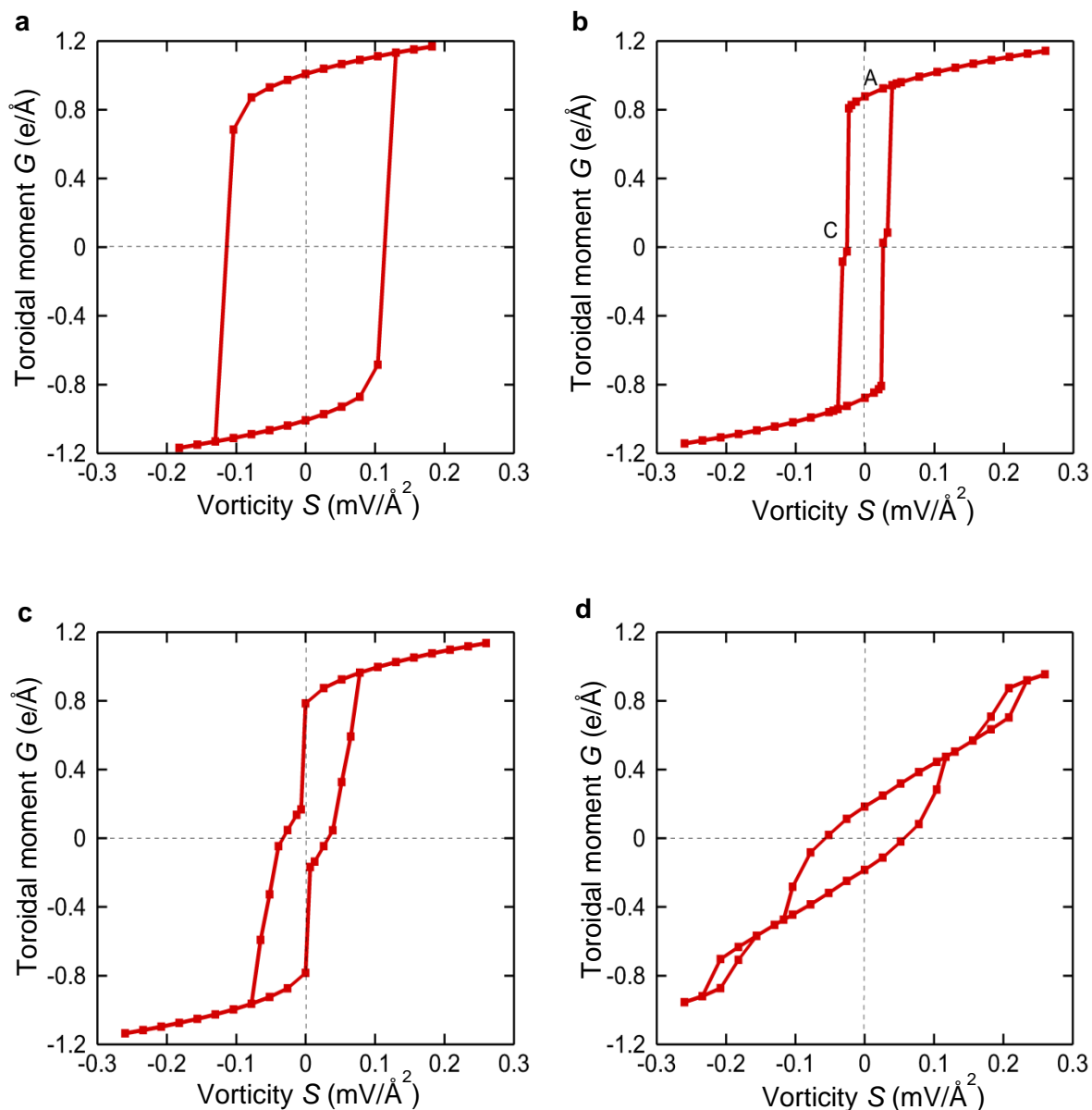


Figure 2 | Hysteresis loops between the toroidal moment G and vorticity S in the ferroelectric memory cell subjected to different compressive strains of ε_{11} , **a** -0.005, **b** -0.01, **c** -0.012, and **d** -0.025. A small compressive strain prefers a single-vortex state, while a large strain induces a multivortex state. The single vortex at point A can be switched to a triple-vortex state at point C by a small vorticity in b, indicating that the multilevel toroidal moments can be controlled by a time-dependent magnetic field.

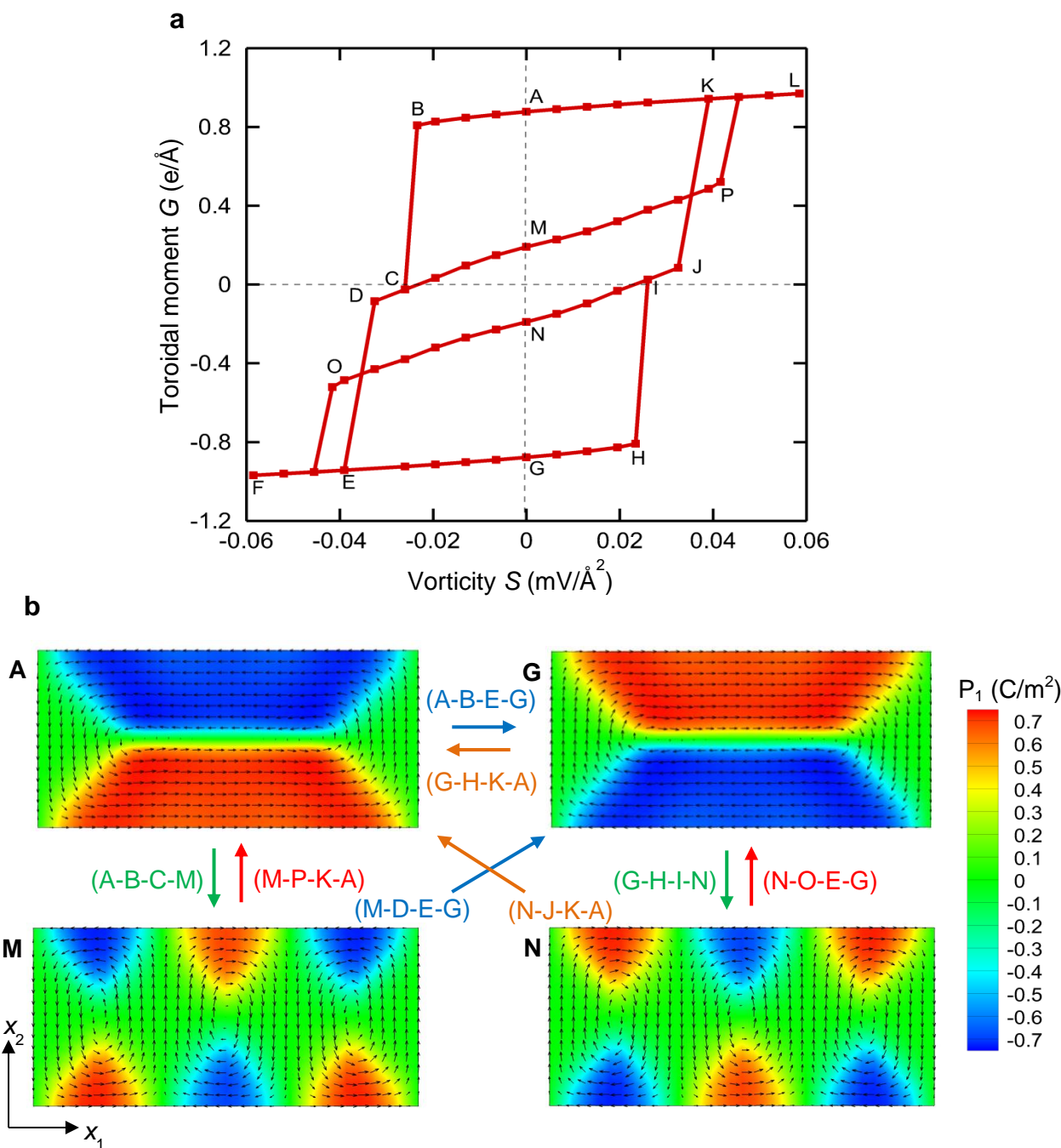


Figure 3 | **a** Three hysteresis loops between the toroidal moment and vorticity in the ferroelectric memory cell subjected to the compressive strain of $\varepsilon_{11}=-0.01$, which are represented by the paths of B-E-H-K, O-F-H-I, and C-P-L-B. **b** Polarization distributions at four stable vortex states at points A, M, N, and G. The four vortex states can be switched from one to the other by a time-dependent magnetic field along different loading paths as shown by the arrows.

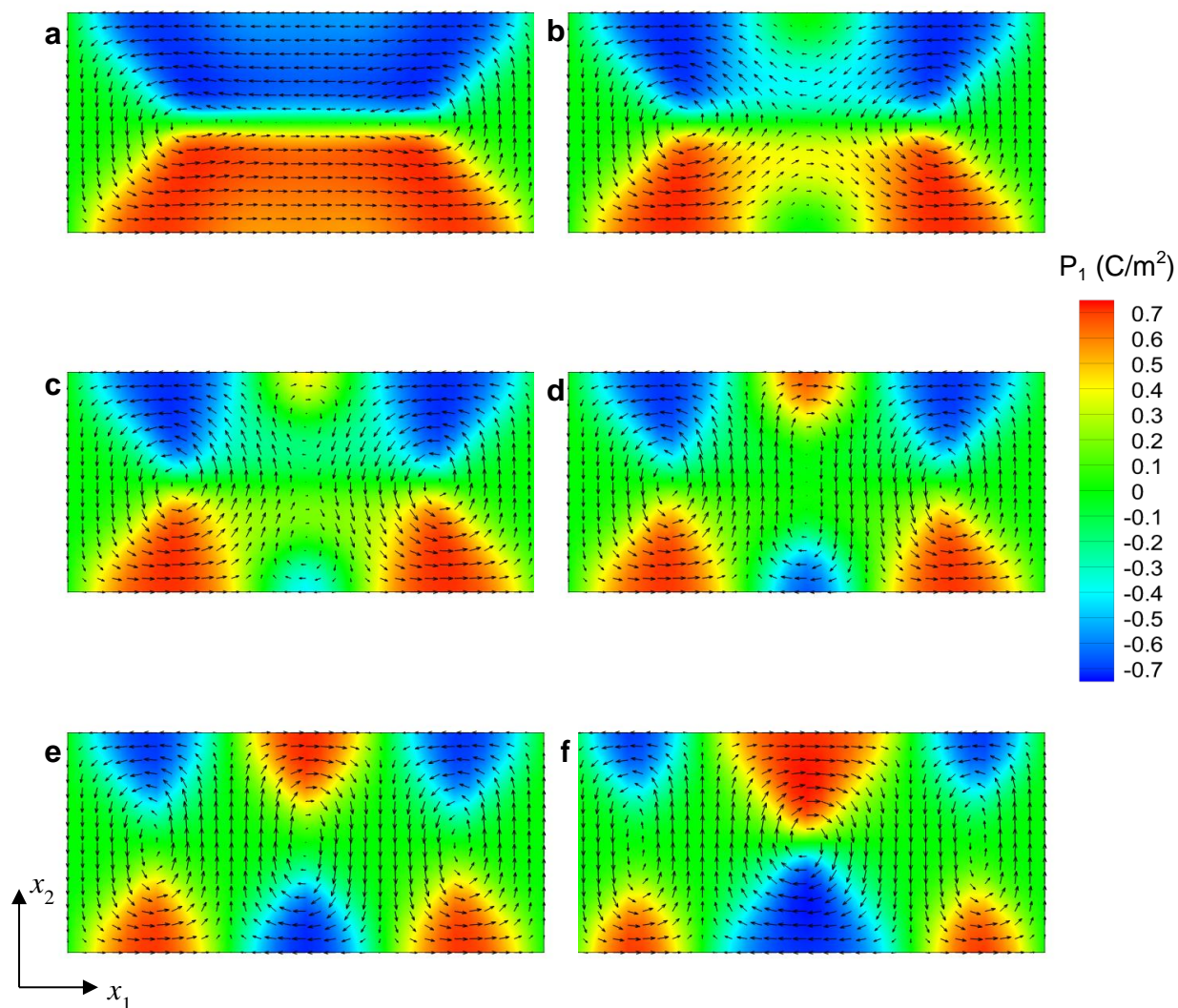


Figure 4 | Domain evolution during the switching from the single-vortex state at point B to the triple-vortex state at point C in Fig. 3a. The switching process is initiated by the disappearance of polarizations at the mid-sections of the upper and lower surfaces, resulting in two vortices with the same circulation formed at the state of **b**. The third vortex was formed following the appearance of opposite polarizations near the mid-sections of the upper and lower surfaces, as shown in **c** and **d**. From **e** to **f**, the middle vortex grows and the switching process is completed.

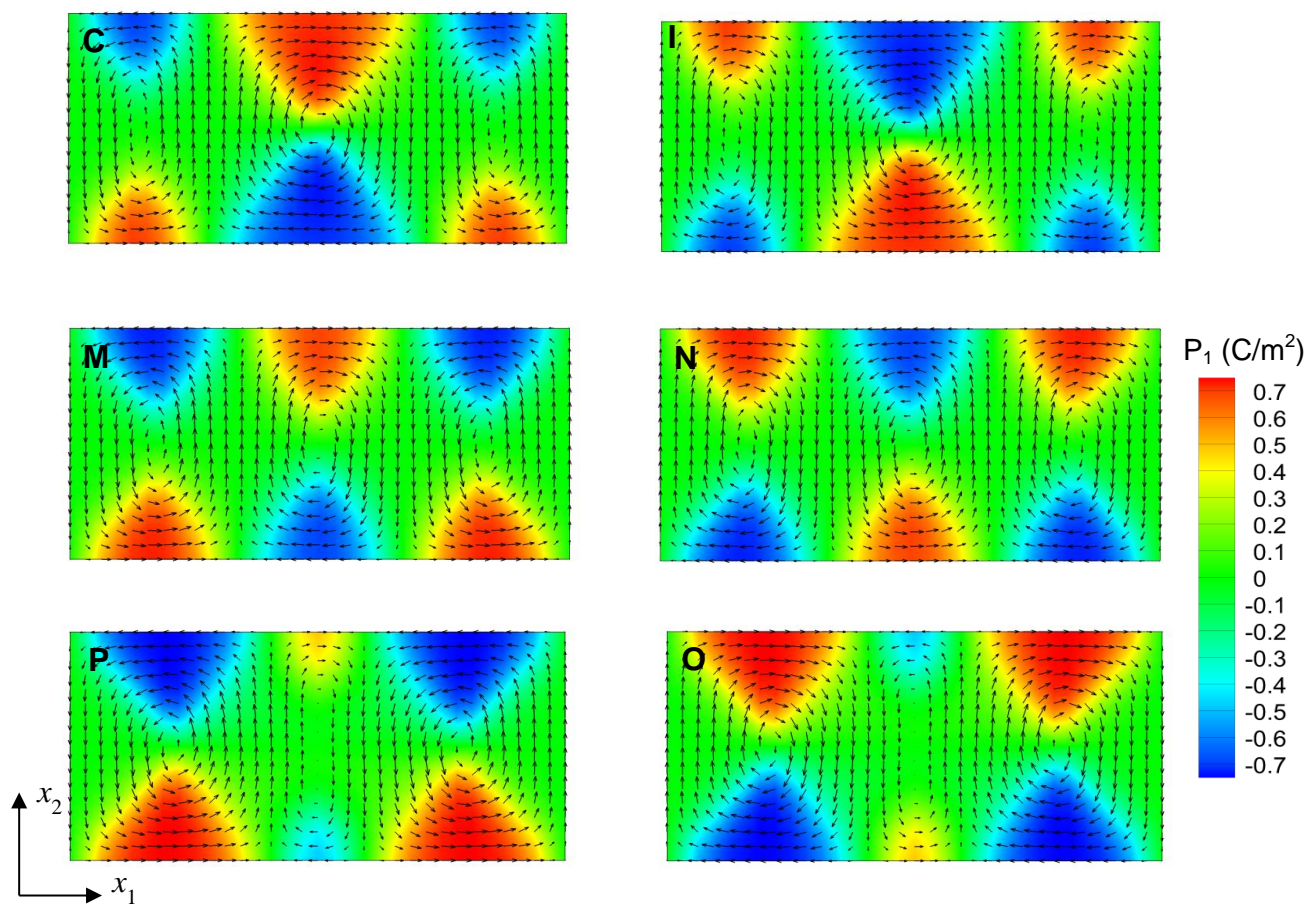


Figure 5 | Detailed domain structures in the triple-vortex states under different vorticities. The left and right panels show the domain evolution along the paths C-M-P and I-N-O in Fig. 3a, respectively. The evolution processes from up to down in both panels are similar, except for the difference of polarization orientations. When the vorticity is zero, the triple vortices exhibit the same size, as shown by the domain structures at points **M** and **N**, and can stably exist in the ferroelectric cell.

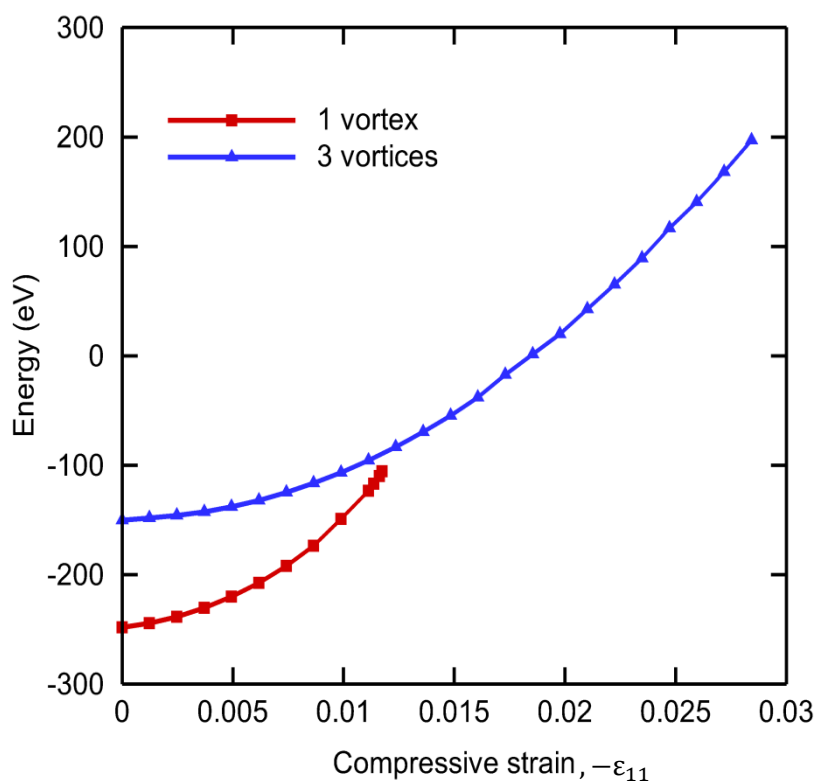


Figure 6 | Strain dependence of total energy for different numbers of vortices in the ferroelectric memory cell. Both the single and triple vortices can exist in the ferroelectric memory cell when the compressive strain ε_{11} is in the range from -0.005 to -0.013. The coexistence of single- and triple-vortex states provides the opportunity to induce the transformation between the different vortex states by the time-dependent magnetic field.